IEEE Access
Multidisciplinary | Rapid Review | Open Access Journal

Received December 16, 2019, accepted December 23, 2019, date of current version January 7, 2020.

Digital Object Identifier 10.1109/ACCESS.2019.2962633

Multiple-Access Interference and Multipath Influence Mitigation for Multicarrier Code-Division Multiple-Access Signals

YUYAO SHEN AND YING XU
Academy of Opto-Electronics, Chinese Academy of Sciences, Beijing 100094, China
Corresponding author: Ying Xu (nadinexy@aoe.ac.cn)

This work was supported in part by the Beijing Natural Science Foundation under Grant 4184108, in part by the National Postdoctoral Program for Innovative Talents under Grant BX201700246, and in part by the Youth Innovation Promotion Association of Chinese Academy of Sciences under Grant Y50301A1BY.

ABSTRACT Sidelobe raising, caused by multipath and multiple-access interference (MAI), hinders the signal detection and time-delay estimation of multicarrier code-division multiple-access (MC-CDMA) signals, which are crucial for localization and tracking applications as well as the sampling-instant configuration of demodulators. Therefore, we propose a method based on reiterative minimum mean-square error (RMMSE) filters to mitigate the MAI and multipath influence. The RMMSE filter is modified to adapt to the multicarrier modulation and symbol involvement characteristics of MC-CDMA signals. The superiority of the proposed method in terms of sidelobes suppression, compared with existing matched filter, least square estimator, least mean square, and single-carrier RMMSE methods, is verified through simulations in the presence of MAIs and short-time-delay multipath. The results show the advantages of the proposed method in terms of high temporal resolution and robustness to MAI influence. This study could contribute toward multipath detection and aid multipath mitigation techniques in strong MAI scenarios.

INDEX TERMS Multicarrier code-division multiple-access (MC-CDMA), multipath, multiple-access interference (MAI), reiterative minimum mean-square error (RMMSE), sidelobes suppression.

I. INTRODUCTION

Code-division multiple-access (CDMA) is a technology extensively used in multiple-access communications as it allows multiple users to use the same spectral resources simultaneously. As an evolution of single-carrier direct sequence spread spectra, multicarrier CDMA (MC-CDMA), combining the advantages of both orthogonal frequency division multiplexing (OFDM) and CDMA technologies to achieve high capacity, spectral efficiency, and anti-jamming capability, is widely used in professional communication systems and exhibits good prospects for both civil and military applications [1]. Signal detection and time-delay estimation of received MC-CDMA signals are crucial not only to localization [2] and tracking applications, but also to the sampling-instant configuration of demodulator. Unfortunately, they are susceptible to the multipath [3] and multiple-access interference (MAI). Multipath components are generated by reflection, scattering, and diffraction from surroundings [4]. MAI is caused by the imperfect-orthogonality among the signature waveforms assigned to multiple-access users [5].

Some methods, such as data-aided precoding [6] and ultra-wide band (UWB) technique [7], have been utilized for suppressing the multipath and MAI influence from the transmitter side. Other studies mitigated interference from the receiver side via antenna design, making use of spatial diversity [8], [9], signal-quality monitoring accompanied with the removal of affected measurements [10], and baseband signal processing, which is introduced in the following paragraphs.

Matched filters accompanied by peak detection are used to indicate the direct path from multipath components in [11]. This classical approach and its derivative methods (such as the matched subspace filters [12]) discard the detailed information of multipath components, such as the number of paths and their time delays, and are confined by its temporal

The associate editor coordinating the review of this manuscript and approving it for publication was Filbert Juwono.

resolution and therefore available only if the paths are well separated. To enhance performance, two efficient implementations of the maximum likelihood technique are proposed in terms of time-delay estimation under multipath situations [1], in which the exact number of paths is utilized in the algorithm design and is therefore required as a priori information. An iterative cleaning process explored recently [13] stresses on eliminating the multipath components which are stronger than direct path components.

Successive interference cancellation [14] and projection methods [15] have been proposed to mitigate MAI. Successive interference cancellation method is a multistage approach that subtracts MAI estimates from the received signal sequentially. This approach and its variation named parallel interference cancellation both require dedicated MAI reproducer and are sensitive to the performance of MAI estimates. Projection method utilizes the orthogonal or quasi-orthogonal property of the signature codes between the desired signal and MAIs.

The studies mentioned above consider MAI and multipath separately. However, given that the coexistence of MAI and multipath leads to an interaction between their disturbances, a collective mitigation method is expected to be better. Deconvolution algorithm based on iterative computations, such as reiterative minimum mean square error (RMMSE) filter based method [16] and least mean square (LMS) method, is a perspective countermeasure to deal with MAI and multipath, considering that it can cope with the sidelobes-distortion caused by.

The RMMSE filter designed adaptively from the received signal using the MMSE principle for each particular discrete time-delay sample has the merits of statistical optimality, capability of sidelobes suppression, and high resolution in the time-delay dimension. Therefore, it has the potential to simultaneously suppress interference from all nearby multipath components and large MAIs. Similar to LMS methods, the RMMSE filter is basically a mean-square error minimization approach and the delay estimate is obtained as the lag time associated with the largest component of the filter. However, it equips with an open-loop structure rather than the popular closed-loop structure used in the LMS method [17]. Therefore, the performance of RMMSE in terms of both robustness and number of required reiterations is better than that of LMS [18]. The multistatic adaptive pulse compression (MAPC) method and its fundamental APC method [19], which are both related to RMMSE, have been developed for range sidelobe suppression directed at radar pulse signals. However, they have restrictions on target signal model and cannot adequately handle MC-CDMA signals, considering the number of subcarriers, symbol involvement, and waveform continuity. Therefore, the conventional MAPC method cannot adequately handle MC-CDMA signals directly.

In this letter, an algorithm based on a modified RMMSE filter is proposed for MC-CDMA signals to suppress the sidelobe raising collectively caused by strong MAI and multipath, and furthermore, to improve the signal detection performance and the ability to distinguish between multipath components. A proper signal model of the MC-CDMA signal is established. Based on this model, we derive and apply a RMMSE filter to each particular time-delay sample, with a particular focus on fitting directed to MC-CDMA signals. Finally, all the theoretical derivations are verified and a performance comparison among the proposed method, matched filter, LMS, least square estimator (LSE), and existing single-carrier RMMSE (SC-RMMSE) [16], [18] are developed by numerical simulations. The results show that the proposed method can adequately handle MC-CDMA signals and outperforms the other three methods in the presence of MAI and multipath.

II. SIGNAL MODEL

The transmitted MC-CDMA signal for the k-th transmitter can be modeled as [20]

$$s_k(t) = \sum_{i=-\infty}^{+\infty} \sum_{n=1}^{N_c} \sum_{m=0}^{L-1} b_{k,n}(i)\, c_k(m) \times p_c\left(\frac{t - mT_c - iT_s}{T_c}\right) e^{j2\pi(f_0 + n\Delta f)t} \quad (1)$$

where N_c and L represent the number of subcarriers and the length of signature code, respectively; $b_{k,n}(i)$ and $c_k(m)$ are the i-th input binary information at the n-th subcarrier and the m-th chip of the spreading code for the k-th transmitter, respectively; T_c and T_s denote the chip duration and symbol duration, respectively; $f_0 + n\Delta f$ is the frequency of the n-th subcarrier; and f_0 and Δf are the fundamental carrier frequency and subcarrier separation, respectively. The pulse waveform $p_c(t)$ is defined as $p_c(t) = 1$ for $0 \le t < 1$ and 0 otherwise. When $\Delta f = L/T_s$, (1) is a multicarrier direct sequence CDMA (MC-DS-CDMA) signal, and when $\Delta f = 1/T_s$, (1) represents a multi-tone (MT) CDMA signal. Both of these cases belong to time domain spreading and multicarrier modulation concepts and are collectively called MC-CDMA [1].

The sampled version of (1) can be represented as

$$s_k(\ell) = \sum_{i=-\infty}^{\infty} \sum_{n=1}^{N_c} \sum_{m=0}^{L-1} b_{k,n}(i)\, c_k(m) \times p_c\left(\frac{\ell/f_s - mT_c - iT_s}{T_c}\right) e^{j2\pi \frac{(f_0 + n\Delta f)}{f_s}\ell} \quad (2)$$

where f_s is the sampling frequency.

The received signal model expressed as a combination of a waveform with known signature and an unknown variable featuring the time-delay information to be estimated is preferred for the convenience of the following derivation of the RMMSE filter. Therefore, we model the received signal in advance. We assumed that without loss of generality, the signals from K transmitters are input simultaneously into the receiver, and each of these signals is propagated over P distinguishable unambiguous paths. Thus, when the complex amplitude corresponds to various time delays as the

kernel function, the ℓ-th sample of the digital baseband received signal is given as

$$\begin{aligned} y(\ell) &= \sum_{k=0}^{K-1}\sum_{i=-\infty}^{\infty}\sum_{n=1}^{N_c}\sum_{p=1}^{P}A_{k,p}\sum_{m'=0}^{L'-1}b_{k,n}(i)c'_k(m') \\ &\quad\times p_c\left(\frac{\ell/f_s-\tau_{k,p}-m'/f_s-iT_s}{1/f_s}\right)e^{j2\pi\frac{n\Delta f}{f_s}(\ell-\tau_{k,p}f_s)} \\ &\quad+v(\ell) \\ &= \sum_{k=0}^{K-1}\sum_{n=1}^{N_c}\sum_{m'=0}^{L'-1}c'_k(m')x_{k,n}\left(\ell-m'\right)e^{j\theta_n m'}+v(\ell) \\ &= \sum_{k=0}^{K-1}\sum_{n=1}^{N_c}\left[\vec{\mathbf{x}}_{k,n}(\ell)\circ\vec{\mathbf{e}}_n\right]^{\mathrm{T}}\vec{\mathbf{c}}_k+v(\ell) \end{aligned} \tag{3}$$

where $A_{k,p}$ and $\tau_{k,p}$ respectively denote the complex amplitude and time delay of the received signal corresponding to the k-th transmitter propagated over the p-th path; $v(\ell)$ is the sampled noise; $\vec{\mathbf{c}}_k = \left[c'_k(0), c'_k(1), \ldots, c'_k\left(L'-1\right)\right]^{\mathrm{T}}$ denotes a vector of spreading code samples corresponding to the k-th transmitter, in which the m'-th element $c'_k(m') = c_k\left(\left\lfloor m'/(T_c f_s)\right\rfloor\right)$ and $\lfloor\cdot\rfloor$ is the round down operator; $L' = LT_c f_s$ is the number of samples within a code period and variable m' denotes the corresponding sample index. For simplicity, L', m', and $c'_k(\cdot)$ are replaced with L, m, and $c_k(\cdot)$ hereafter, respectively. The operator "$\circ$" and superscript "T" denote the Hadamard product and transpose operation, respectively. The term $x_{k,n}(\ell)$ denotes the complex amplitude corresponding to the ℓ-th sample in the time-delay dimension, which can be expressed as

$$\begin{aligned} x_{k,n}(\ell) &= \sum_{i=-\infty}^{\infty}\sum_{p=1}^{P}A_{k,p}b_{k,n}(i)e^{j2\pi\frac{n\Delta f}{f_s}(\ell-\tau_{k,p}f_s)} \\ &\quad\times p_c\left(\frac{\ell/f_s-iT_s-\tau_{k,p}}{1/f_s}\right) \\ &= \begin{cases} A_{k,p}b_{k,n}(i)\,e^{j\theta_n iT_s f_s}, & \ell = iT_s f_s+\tau_{k,p}f_s \\ \qquad\text{where } i\in\mathbb{Z} \text{ and } p=1,2,\ldots,P & \\ 0, \qquad\qquad\text{others} & \end{cases} \end{aligned} \tag{4}$$

Herein, $\mathbb{Z}$ stands for the set of integers. In this way, the complex amplitude samples are dichotomized into two categories according to their values, i.e., nonzero ones and the others. The nonzero complex amplitude samples have indices of ℓs that correspond to the time delay of the preset P different propagating paths, i.e., $\tau_{k,p}$, $p = 1, 2, \ldots, P$. Term $iT_s f_s$ in the expression of index ℓ corresponding to nonzero $x_{k,n}(\ell)$ means that ℓ locates in the i-th input binary information duration. Value i only has effect on the symbol sign of nonzero $x_{k,n}(\ell)$ and an additional phase shift.

The L-dimensional vector $\vec{\mathbf{x}}_{k,n}(\ell)$ is defined as

$$\vec{\mathbf{x}}_{k,n}(\ell) = \left[x_{k,n}(\ell)\;\; x_{k,n}(\ell-1)\cdots x_{k,n}(\ell-L+1)\right]^{\mathrm{T}}. \tag{5}$$

According to the above analysis of $x_{k,n}(\ell)$. The number of nonzero elements in $\vec{\mathbf{x}}_{k,n}(\ell)$ and the corresponding index respectively indicate the number of propagating paths and the corresponding time delay. The vector $\vec{\mathbf{e}}_n = \left[1,\; e^{j\theta_n},\ldots,e^{j(L-1)\theta_n}\right]^{\mathrm{T}}$ represents the relative phase-shifts of L contiguous samples in $\vec{\mathbf{x}}_{k,n}(\ell)$, where $\theta_n = 2\pi n\Delta f/f_s$ is the phase-shift between successive received samples of the n-th subcarrier.

By moving the Hadamard product with the phase-shifts $\vec{\mathbf{e}}_n$ from the vector $\vec{\mathbf{x}}_{k,n}(\ell)$ to vector $\vec{\mathbf{c}}_k$, (3) can be rewritten as

$$y(\ell) = \sum_{k=0}^{K-1}\sum_{n=1}^{N_c}\vec{\mathbf{x}}_{k,n}^{\mathrm{T}}(\ell)\,\vec{\mathbf{c}}_{k,n}+v(\ell) \tag{6}$$

where $\vec{\mathbf{c}}_{k,n} = \vec{\mathbf{c}}_k\circ\vec{\mathbf{e}}_n = \left[c_{k,n}(0), c_{k,n}(1), \ldots, c_{k,n}(L-1)\right]^{\mathrm{T}}$ is a frequency-shifted version of the code samples, and $c_{k,n}(m) = c_k(m)\,e^{jm\theta_n T_c f_s}$. Thus, the received signal denoted by (3) can be regarded as a summation of KN_c different signals. There is no explicit representation of time delay in the derived signal model (6), which is the same as the reverberation model described in [21].

The vector consisting of L contiguous received signal samples can be represented as

$$\vec{\mathbf{y}}(\ell) = [y(\ell)\;\; y(\ell+1)\cdots y(\ell+L-1)]^{\mathrm{T}} \tag{7}$$

then

$$\vec{\mathbf{y}}(\ell) = \sum_{k=0}^{K-1}\sum_{n=1}^{N_c}\mathbf{X}_{k,n}^{\mathrm{T}}(\ell)\,\vec{\mathbf{c}}_{k,n}+\vec{\mathbf{v}}(\ell) \tag{8}$$

where $\mathbf{X}_{k,n}(\ell)\in\mathbb{C}^{L\times L}$ is the matrix consisting of complex amplitude samples corresponding to various time delays, denoted as $\left[\vec{\mathbf{x}}_{k,n}(\ell)\;\; \vec{\mathbf{x}}_{k,n}(\ell+1)\;\cdots\;\vec{\mathbf{x}}_{k,n}(\ell+L-1)\right]$. $\vec{\mathbf{y}}(l)$, $\vec{\mathbf{c}}_{k,n}$, $\vec{\mathbf{v}}(l)\in\mathbb{C}^L$ and the noise vector $\vec{\mathbf{v}}(l) = [v(l)\;\; v(l+1)\;\cdots v(l+L-1)]^{\mathrm{T}}$.

When the signal for the k-th transmitter is configured as the desired signal, the other $K-1$ signals are MAIs. Besides, the properties of the elements in $\mathbf{X}_{k,n}$ can be concluded as follows: 1) in situations free from multipath influence, the time delay can be derived from the index of nonzero element in $\mathbf{X}_{k,n}$; 2) in multipath situations, the time delay of the direct path and the distance between the transmitter and receiver can be derived from the index of the first nonzero element in $\mathbf{X}_{k,n}$; the other nonzero elements indicate the multipath components. Thus, signal detection and time-delay estimates can be obtained by matrix $\mathbf{X}_{k,n}$ estimation, in which a RMMSE-based method can be used to mitigate the MAI and multipath influence collectively. Detailed information regarding this is provided in the following section.

III. PROPOSED METHOD

In this section, we proposed an RMMSE method based on the derived MC-CDMA signal model to collectively mitigate MAI and multipath influence.

The complex amplitude estimate obtained using an RMMSE filter is denoted by $\hat{x}_{k,n}(\ell) = \vec{\mathbf{w}}_{k,n}^{\mathrm{H}}(\ell)\,\vec{\mathbf{y}}(\ell)$, in which $\vec{\mathbf{w}}_{k,n}(\ell) = \left[w_{k,n}(\ell)\cdots w_{k,n}(\ell+L-1)\right]^{\mathrm{T}}\in\mathbb{C}^L$

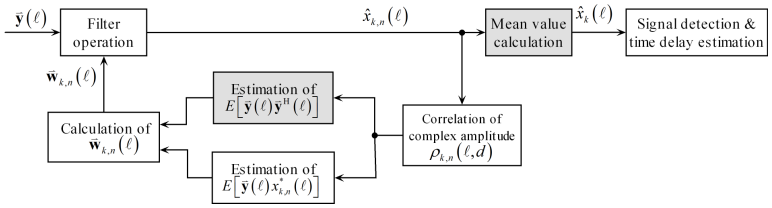

FIGURE 1. Schematic of the modified reiterative minimum mean-square error (RMMSE) algorithm.

is the vector of the weight coefficients of the RMMSE filter, in which the superscript "H" stands for the conjugate transpose. To completely utilize the correlation properties of the spreading code, the filter order is generally configured the same as the number of spreading code samples (i.e., L). The derivation of the coefficients $\vec{\mathbf{w}}_{k,n}(\ell)$ is crucial to the RMMSE method. The MMSE cost function [18] is $J_{k,n}(\ell) = E\left[\left|x_{k,n}(\ell) - \vec{\mathbf{w}}_{k,n}^{\mathrm{H}}(\ell)\,\vec{\mathbf{y}}(\ell)\right|^2\right]$, in which the operator "E" is used to represent the expected operation. Therein, by minimizing $J_{k,n}(\ell)$, we can have

$$\vec{\mathbf{w}}_{k,n}(\ell) = \left(E\left[\vec{\mathbf{y}}(\ell)\,\vec{\mathbf{y}}^{\mathrm{H}}(\ell)\right]\right)^{-1} E\left[\vec{\mathbf{y}}(\ell)\,x_{k,n}^{*}(\ell)\right] \tag{9}$$

where superscript "*" is the conjugation operation.

Furthermore, the cross-correlation and autocorrelation functions can be derived respectively as

$$E\left[\vec{\mathbf{y}}(\ell)\,x_{k,n}^{*}(\ell)\right] = \rho_{k,n}(\ell,0)\,\vec{\mathbf{c}}_{k,n} \tag{10}$$

and

$$\begin{aligned}
&E\left[\vec{\mathbf{y}}(\ell)\,\vec{\mathbf{y}}^{\mathrm{H}}(\ell)\right] \\
&= \sum_{k=0}^{K-1}\sum_{n=1}^{N_c} E\left[\mathbf{X}_{k,n}^{\mathrm{T}}(\ell)\,\vec{\mathbf{c}}_{k,n}\vec{\mathbf{c}}_{k,n}^{\mathrm{H}}\mathbf{X}_{k,n}^{*}(\ell)\right] + \sigma^2\mathbf{I}_L \\
&= \sum_{k=0}^{K-1}\sum_{n=1}^{N_c}\left[\sum_{j=-L+1}^{L-1}\rho_{k,n}(\ell+j,0)\,\vec{\mathbf{c}}_{k,n}(j)\,\vec{\mathbf{c}}_{k,n}^{\mathrm{H}}(j)\right. \\
&\quad + \sum_{j=1}^{L-1}\rho_{k,n}(\ell+j,-L)\,\vec{\mathbf{c}}_{k,n}(j)\,\vec{\mathbf{c}}_{k,n}^{\mathrm{H}}(-L+j) \\
&\quad \left. + \sum_{j=-L+1}^{-1}\rho_{k,n}(\ell+j,L)\,\vec{\mathbf{c}}_{k,n}(j)\,\vec{\mathbf{c}}_{k,n}^{\mathrm{H}}(L+j)\right] + \sigma^2\mathbf{I}_L
\end{aligned} \tag{11}$$

where $\rho_{k,n}(\ell,d) = E\left[x_{k,n}(\ell)\,x_{k,n}^{*}(\ell+d)\right]$ denotes the correlation function of $x_{k,n}(\ell)$ and $\mathbf{I}_L$ is the $L \times L$ scaled unit matrix. It should be noted that in the derivation of (11), the orthogonality between subcarriers and the correlation characteristics of the elements in $\mathbf{X}_{k,n}(\ell)$ are utilized. The detailed correlation characteristics are summarized concretely as follows:

1) Similar assumptions underly existing RMMSE methods [19]: first, the amplitude samples are uncorrelated with noise components (i.e., $E\left[x_{k,n}(\ell)\,v^{*}(\hbar)\right] = 0$); second, the amplitude samples corresponding to different transmitters are uncorrelated (i.e., $E\left[x_{k,n}(\ell)\,x_{m,n}^{*}(\hbar)\right] = 0$, where $k \neq m$, ℓ and $\hbar$ are arbitrary integers).

2) Modified assumptions according to the specific signal modulation: in terms of radar pulse signal shown in [10], $E\left[x_k(\ell)\,x_k^{*}(\hbar)\right] = 0$ where $\ell \neq \hbar$; in terms of direct-sequence spread spectrum (DSSS) signal with low data rate shown in [12], $E\left[x_k(\ell)\,x_k^{*}(\ell+d)\right] = E\left[|x_k(\ell)|^2\right]$ when d is an integer multiple of L and 0 otherwise; in terms of an MC-CDMA signal with a low data rate, there is an identical phase error between the elements in $\mathbf{X}_{k,n}(\ell)$ with a time delay of a certain times of L, and thus $E\left[x_{k,n}(\ell)\,x_{k,n}^{*}(\ell+d)\right] = E\left[\left|x_{k,n}(\ell)\right|^2 e^{-j\theta_n dT_c f_s}\right]$ if $d \in \{\pm L, 0\}$ and 0 otherwise; in terms of an MC-CDMA signal with a high data rate, the correlation between the elements in $\mathbf{X}_{k,n}(\ell)$ with a time delay of integer multiple L is destroyed by the quasi-orthogonality of randomly distributed symbol signs, and therefore $E\left[x_{k,n}(\ell)\,x_{k,n}^{*}(\ell+d)\right] = E\left[\left|x_{k,n}(\ell)\right|^2\right]$ if $d = 0$ and 0 otherwise. In addition, the complex amplitude samples in an MC-CDMA signal corresponding to different subcarriers are uncorrelated owing to the quasi-orthogonality of randomly distributed symbol signs modulated, and therefore, $E\left[x_{k,n}(\ell)\,x_{k,m}^{*}(\hbar)\right] = 0$, where $n \neq m$, and ℓ and $\hbar$ are arbitrary integers. In conclusion, the coefficients of RMMSE filters corresponding to different signal models are different from each other.

The modified RMMSE algorithm is represented in Fig. 1. The main difference between the modified RMMSE and the existing ones [16], [18] is highlighted by the dark blocks, including the estimation of autocorrelation function $E\left[\vec{\mathbf{y}}(\ell)\,\vec{\mathbf{y}}^{\mathrm{H}}(\ell)\right]$ and the mean value calculation. The former was modified based on the specific correlation characteristics; the latter was added to achieve a diversity gain caused by subcarrier allocation. Its pseudo code is presented in **Algorithm 1**. Herein, parameter N_r denotes the number of reiterations of the proposed algorithm, whose empirical value is usually 4-10 and can be determined specifically by simulations. It is less than the reiteration number of the approaches with closed-loop structure, such as LMS, benefiting from the open-loop structure. By filtering the received signals utilizing the modified RMMSE adaptive

filter, the complex amplitude estimates mitigating the MAI and multipath influence are obtained. This in turn helps improve the performance of signal detection and time-delay estimation.

Algorithm 1 Proposed Multiple-Access Interference (MAI) and Multipath Mitigation Method

1: $\hat{x}_{k,n}(\ell) = 1$, $k = 0$ to $K-1$, $n = 1$ to N_c, and $-N_r(L-1) < \ell < (N_r+1)(L-1)$;
2: **for** $i = 1$ to N_r **do**
3: **for** $k = 0$ to $K-1$ **do**
4: **for** $n = 1$ to N_c **do**
5: $\rho_{k,n}(\ell, d) = \hat{x}_{k,n}(\ell)\hat{x}^*_{k,n}(\ell+d)$, $d = -L, 0, L$
6: compute $\vec{\mathbf{w}}_{k,n}(\ell)$,$-(N_r-i)(L-1) < \ell < (N_r+1-i)(L-1)$ using equation (9), (10), and (11);
7: update $\hat{x}_{k,n}(\ell)$ using $\hat{x}_{k,n}(\ell) = \vec{\mathbf{w}}^{\mathrm{H}}_{k,n}(\ell)\,\vec{\mathbf{y}}(\ell)$;
8: **end for**
9: **end for**
10: **end for**
11: calculate $\hat{x}_k(\ell)$ by $\hat{x}_k(\ell) = \left(\sum_{n=1}^{N_c}\left|\hat{x}_{k,n}(\ell)\right|\right)\Big/N_c$

The performance of the proposed algorithm depends on the produced statistics. Their joint probability density function is difficult to obtain [22]; thus, apart from theoretical derivations, the performance of the adaptive filter is examined using the empirical statistics obtained by simulations as in [18] and [19], as discussed in the following section.

According to [23], computational loads were examined in Table 1. Among the listed five methods, the matched filter is apparently the simplest. In comparison, the complexity of LSE is slightly higher, even with pre-calculated filter coefficients. However, these two methods are only appropriate for solo-transmitter applications and perform poorly in the presence of MAIs [19]. SC-RMMSE and the proposed method calculate the filter coefficients function via direct matrix inversion; therefore, they demand more computational complexity. Furthermore, the complexity of the proposed algorithm is about N_c times higher than the SC-RMMSE methods, in order to achieve a diversity gain caused by subcarrier allocation. LMS is based on the steepest gradient descent algorithm to correct the filter coefficients iteratively for achieving the optimum result, and thus reduces complexity. However, this advantage is achieved at the expense of convergence rate and filter performance, especially when the signal is corrupted by strong interference.

IV. NUMERICAL RESULTS

Simulations were conducted to examine the validity the derived signal model and the sidelobe-suppression performance of the proposed algorithm. The simulation conditions are listed in Table 2.

TABLE 1. Computational requirement.

Filter	Number of Operations
Matched filter	$\mathcal{O}(LN_cN_\tau{}^{\dagger})$
LSE	$\mathcal{O}(LN_cN_\tau + N_\tau^2N_c)$
LMS	$\mathcal{O}(LN_rN_cKN_\tau + N_{SF}{}^{\dagger\dagger})$
SC-RMMSE	$\mathcal{O}(L^3N_rKN_\tau)$
Proposed method	$\mathcal{O}(L^3N_rN_cKN_\tau)$

† N_τ is the length of processing window in the time-delay dimension.
†† N_{SF} denotes the number of multiplications used for the calculation of the optimal configuration of step factor for LMS method.

TABLE 2. Simulation conditions.

Parameter	Value	Unit
Code rate	63	kcps
Code length	63	chip
Code period	1	ms
MAI-to-signal power ratio	10	dB
Sample frequency	200	kHz
Symbol rate	1	kbps
Multipath fading	5	dB
Number of subcarriers	5	-

A. SIGNAL MODEL VALIDATION

Noiseless signals were generated according to the derived signal expression in (8) and the commonly used signal model shown as (1). Both MC-DS-CDMA ($\Delta f = 63$ kHz) and MT-CDMA ($\Delta f = 1$ kHz) signals are examined, where $K = 3$ and $P = 2$, respectively. The simulated signal waveforms with a decimation factor of 3 are shown in Fig. 2. The decimation operation is solely for visualization and not intended for the following signal processing operations. The difference between the signals generated according to the proposed signal expression and reference signals are always 0 as shown in Fig. 2(c) and (f). Therefore, the derived MC-CDMA signal model is validated in the presence of the multipath and MAI. It provides a foundation to investigate the MAI and multipath mitigation algorithm for MC-CDMA signals.

B. MAI AND MULTIPATH MITIGATION PERFORMANCE

In this subsection, MC-DS-CDMA is selected without loss of generality as the object of simulations to evaluate the performance of the proposed RMMSE method. The integration time is configured as 1 ms.

The number of reiterations required for the proposed algorithm N_r, was initially investigated via simulations. The peak value of normalized complex amplitude estimates obtained under different N_r is selected as an indicator, denoted by $\max_{\ell}\left\{10\log_{10}\left(\left|\hat{x}(\ell)^2\right|/P_n\right)\right\}$ in Fig.3. A Monte Carlo simulation was performed under a pre-detection signal-to-noise ratio (SNR) [24] of 15 dB, and the results were obtained under 50 runs. Three typical situations were explored, as illustrated in the legend. Situation "$K = 1, P = 1$" represents that only the direct path signal from the desired transmitter is received; situation "$K = 1, P = 2$" denotes the simulation developed in the presence of a multipath component with a

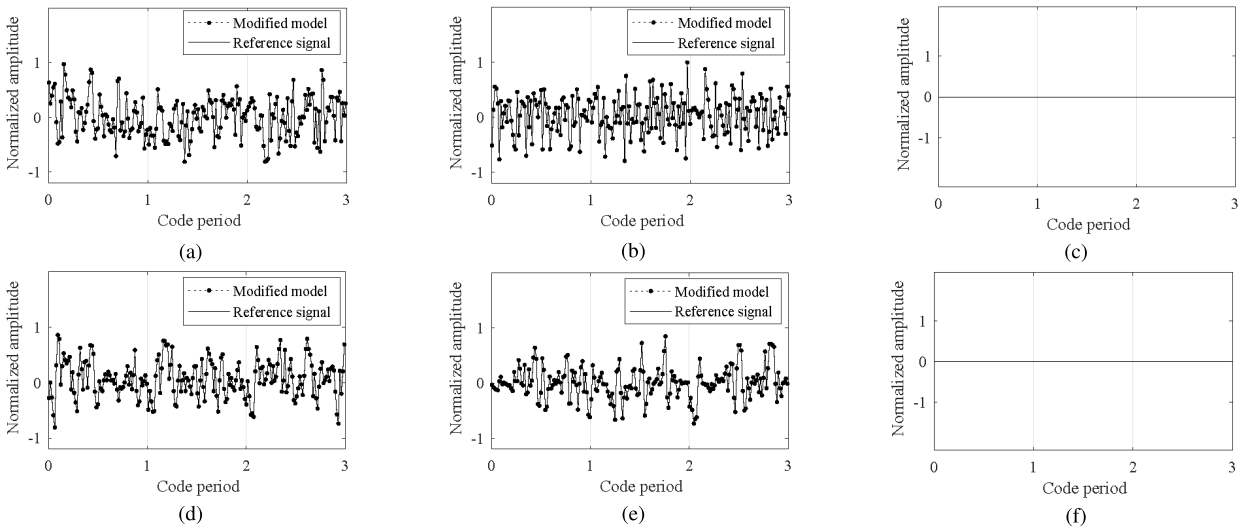

FIGURE 2. $K = 3$ and $P = 2$ signals generated by derived and reference signal models and their difference: (a) Real part, MC-DS-CDMA. (b) Imaginary part, MC-DS-CDMA. (c) Bias, MC-DS-CDMA. (d) Real part, MT-CDMA. (e) Imaginary part, MT-CDMA. (f) Bias, MT-CDMA.

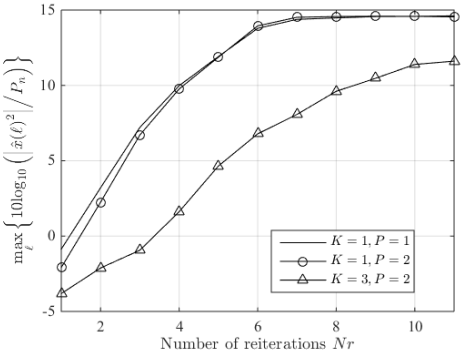

FIGURE 3. The peak value of normalized complex amplitude estimates under different N_r.

delay of 0.954 chip; and situation "$K = 3, P = 2$" represents a corrupted direct-path signal by a multipath component and two strong MAIs. The simulation results show that the obtained statistics grow with the increase of N_r. However, when $N_r \geqslant 6$, the growth tends to slow for the condition that $K = 1$; while for the condition that $K = 3$, the critical point is $N_r = 10$.

In the following simulations, the proposed method is examined in comparison to the existing matched filter, LMS, LSE, and SC-RMMSE methods. According to the investigation above, the RMMSE-based methods reiterate 6 and 10 times respectively for MAI absence and presence scenarios, whereas the number of recursions of LMS method is configured as 100 which is ten times higher.

The simulated results for normalized complex amplitude estimates are illustrated in Fig. 4. Fig. 4(a) is obtained in noise-free environments and the corresponding normalized complex amplitude is obtained from the desired signal. Other figures are obtained under an SNR of 15 dB, and the normalized complex amplitude is obtained from the noise power. The X-axis indicates the time delay normalized by the code period; a locally enlarged image is attached for each subfigure. As shown in Fig. 4(a), the peak locations of the complex amplitude estimates obtained by the existing four methods all coincide with the preset target location marked by a dash-dot line labeled "T", when there is neither multipath nor MAI. The simulated results obtained by the proposed method points to the same conclusion; furthermore, we obtained much lower sidelobes. Fig. 4(b) illustrates that LSE method becomes invalid due to the corruption by noise, while other methods remain effective. Therefore, the LSE method was no longer examined in the following simulations. The simulation result shown in Fig. 4(c) implies that the multipath component cannot be correctly detected by the matched filter. In contrast, the locations of the secondary peak obtained by the other three methods coincide with the preset time-delay of the multipath component, marked by a dash-dot line labeled "MultiPath." The proposed method performs the best in terms of the sidelobe mitigation. Therefore, the improvement in ability of the proposed method to distinguish between the direct path signal and the multipath component is verified. Additionally, as shown in Fig. 4(d), with the involvement of multipath and strong MAIs, the sidelobe level of the matched filter output increases greatly and overwhelms the expected peak of the direct path signal and multipath component. Similarly, the performance of SC-RMMSE method degrades dramatically and abnormal large sidelobes yield in this situation, since SC-RMMSE can barely cope with one of the subcarriers of MAI while ignoring the influence of the others. In contrast, accurate time-delay estimates of the direct path signal and the multipath component can be still obtained using the results of the proposed method in presence of MAI and multipath; and the sidelobe level of the proposed method is much lower than that of the other three methods, which reveals its ability

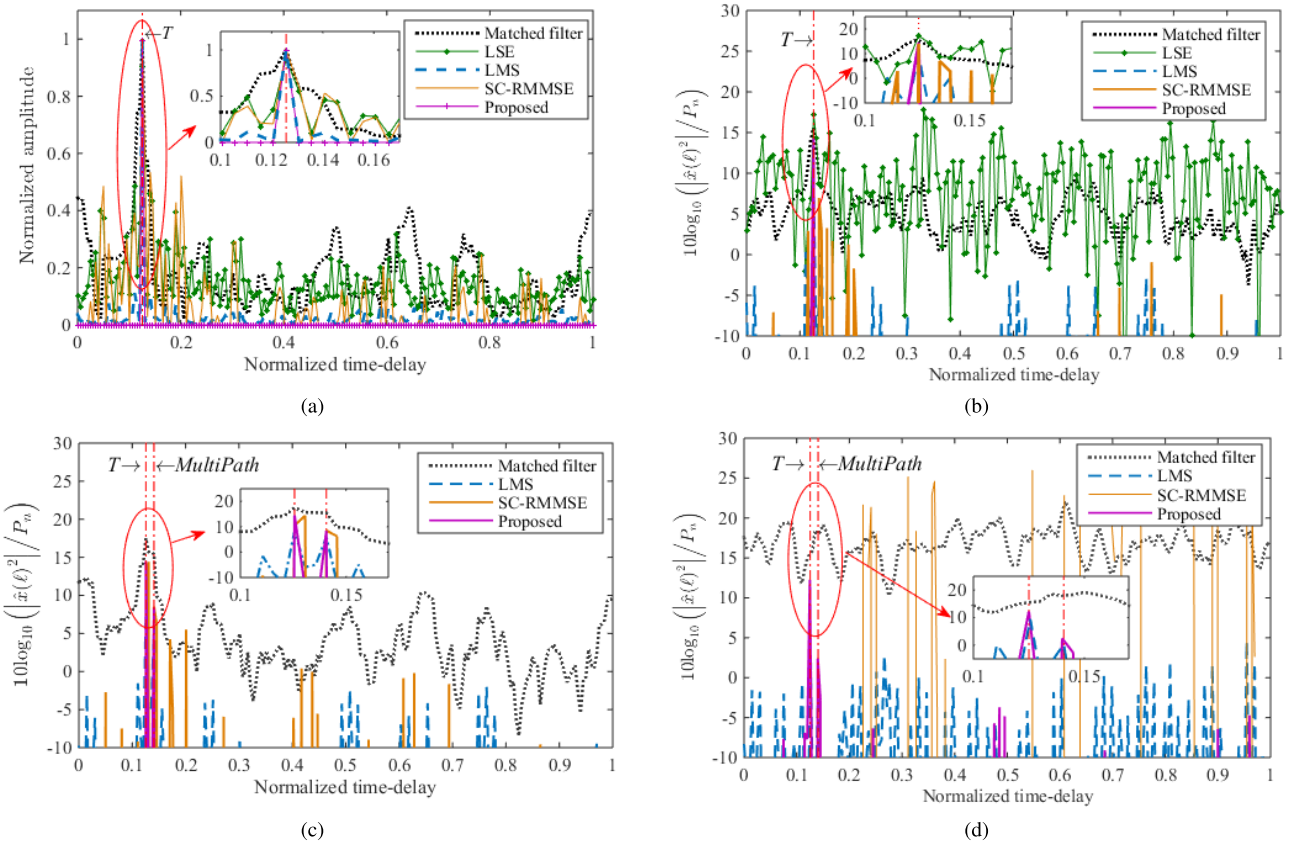

FIGURE 4. Complex amplitude estimates with and without multiple-access interference (MAI) and multipath: (a) $K = 1$ and $P = 1$, free from noise. (b) $K = 1$ and $P = 1$. (c) $K = 1$ and $P = 2$. (d) $K = 3$ and $P = 2$.

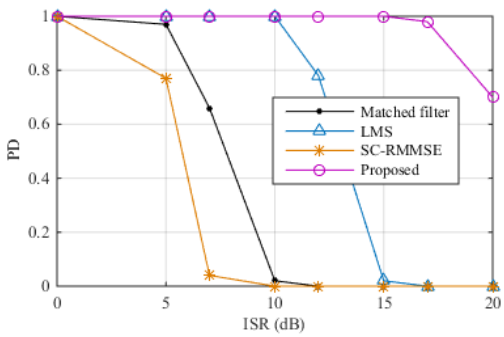

FIGURE 5. Interference mitigation performance under various multiple-access interference-to-signal power ratio (ISR) situations.

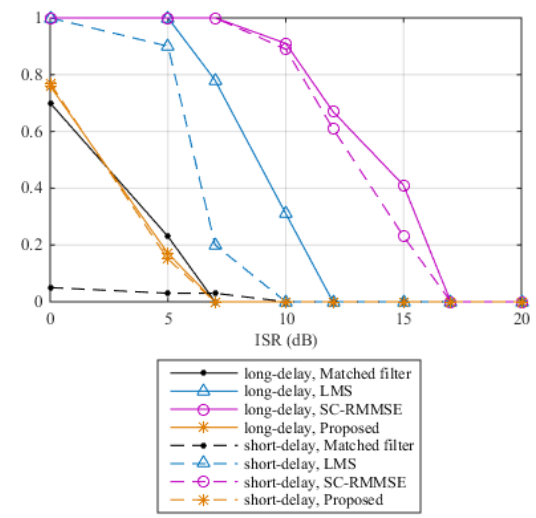

FIGURE 6. Multipath detection probability when $K = 3$ and $P = 2$.

to reduce sidelobes caused by the MAI and short-time-delay multipath.

Similar conclusions can be drawn upon examining the peak location detection probability (PD), shown in Fig. 5. In view of the sensitivity of LSE to SNR, only the matched filter, LMS, SC-RMMSE, and the proposed method are examined hereafter. When the MAI-to-signal power ratio (ISR) is larger than 10 dB, the PD results of matched filter, LMS, and SC-RMMSE decrease greatly and drop to be zero. This means that the expected peak of the desired signal is overwhelmed by the sidelobes of the multipath fading channel and strong MAIs, and hence cannot be detected. In contrast, the proposed method performs well.

Furthermore, the multipath detection performance is examined through simulations in both short- (0.945 chip) and long-delay (10.08 chips) multipath scenarios. The results in Fig. 6 indicate that the multipath detection

probability (MPD) drops as the ISR of MAI increases. The proposed method is superior than the matched filter, LMS, and SC-RMMSE methods in terms of the MPD; further, the superiority is more significant for short-delay multipath scenarios. Herein, as the lag time shortens, the direct path and multipath components of the matched filter output merge into one peak, which hinders the multipath detection even in low ISR condition.

V. CONCLUSION

A method based on the RMMSE filter is proposed to mitigate the MAI and multipath influence for MC-CDMA signals. The RMMSE filter is modified for better adaptability to multicarrier modulation and symbol involvement characteristics. Numerical results show that the proposed method has superiority in respect to sidelobes suppression, as compared with the existing matched filter, LMS, LSE, and SC-RMMSE methods in large MAI and multipath scenarios. The improvement in terms of the detection performance of the direct path signal and the ability to distinguish multipath components are both verified by simulations. This study provides a new perspective to solve MAI and multipath problems in future professional communication systems, and in ranging and navigation applications using MC-CDMA signals. The dynamic robustness of the proposed method and complexity reduction will be the focus of future work.

REFERENCES

[1] A. Masmoudi, F. Bellili, S. Affes, and A. Ghrayeb, "Maximum likelihood time delay estimation from single- and multi–carrier DSSS multipath MIMO transmissions for future 5G networks," *IEEE Trans. Wireless Commun.*, vol. 16, no. 8, pp. 4851–4865, Aug. 2017.

[2] M. Einemo and H. C. So, "Weighted least squares algorithm for target localization in distributed MIMO radar," *Signal Process.*, vol. 115, pp. 144–150, Oct. 2015.

[3] A. Scaloni, P. Cirella, M. Sgheiz, R. Diamanti, and D. Micheli, "Multipath and Doppler characterization of an electromagnetic environment by massive MDT measurements from 3g and 4g mobile terminals," *IEEE Access*, vol. 7, pp. 13024–13034, 2019.

[4] Z. Huang, R. Zhang, J. Pan, Y. Jiang, and D. Zhai, "A framework of multipath clustering based on space–transformed fuzzy c-means and data fusion for radio channel modeling," *IEEE Trans. Veh. Technol.*, to be published, doi: 10.1109/tvt.2019.2947605.

[5] J. Yang and R. C. De Lamare, "Widely-linear minimum-mean-squared error multiple-candidate successive interference cancellation for multiple access interference and jamming suppression in direct-sequence code-division multiple-access systems," *IET Signal Process.*, vol. 9, no. 1, pp. 73–81, Feb. 2015.

[6] Y. Choi, J. Lee, M. Rim, and C. G. Kang, "Constructive interference optimization for data–aided precoding in multi–user MISO systems," *IEEE Trans. Wireless Commun.*, vol. 18, no. 2, pp. 1128–1141, Feb. 2019.

[7] S. Wang, G. Mao, and J. A. Zhang, "Joint time-of-arrival estimation for coherent UWB ranging in multipath environment with multi–user interference," *IEEE Trans. Signal Process.*, vol. 67, no. 14, pp. 3743–3755, Jul. 2019.

[8] H.-H. Chen and J.-S. Lee, "Adaptive joint beamforming and B-MMSE detection for CDMA signal reception under multipath interference," *Int. J. Commun. Syst.*, vol. 17, no. 7, pp. 705–721, Sep. 2004.

[9] J. Wu, X. Tang, Z. Li, C. Li, and F. Wang, "Cascaded interference and multipath suppression method using array antenna for GNSS receiver," *IEEE Access*, vol. 7, pp. 69274–69282, May 2019.

[10] A. Pirsiavash, A. Broumandan, and G. Lachapelle, "Characterization of signal quality monitoring techniques for multipath detection in GNSS applications," *Sensors*, vol. 17, no. 7, p. 1579, Jul. 2017.

[11] J. Veen and P. Van Der Wiellen, "The application of matched filters to PD detection and localization," *IEEE Electr. Insul. Mag.*, vol. 19, no. 5, pp. 20–26, Sep. 2003.

[12] S. Korkmaz and A.-J. Van Der Veen, "Time delay estimation in dense multipath with matched subspace filters," in *Proc. Workshop Positioning, Navigat. Commun.*, Hanover, Germany, May 2008.

[13] L. Zhang, M. Chen, X. Wang, and Z. Wang, "TOA estimation of chirp signal in dense multipath environment for low–cost acoustic ranging," *IEEE Trans. Instrum. Meas.*, vol. 68, no. 2, pp. 355–367, Feb. 2019.

[14] A. Maatouk, E. Caliskan, M. Koca, M. Assaad, G. Gui, and H. Sari, "Frequency–domain NOMA with two sets of orthogonal signal waveforms," *IEEE Commun. Lett.*, vol. 22, no. 5, pp. 906–909, May 2018.

[15] D. Zhang, K. Wang, and X. Zhang, "Blind adaptive affine projection algorithm-based multiuser detector over a multipath fading channel," *Signal Process.*, vol. 90, no. 6, pp. 2102–2106, Jun. 2010.

[16] T. D. Cuprak and K. E. Wage, "Efficient Doppler–compensated reiterative minimum mean-squared-error processing," *IEEE Trans. Aerosp. Electron. Syst.*, vol. 53, no. 2, pp. 562–574, Apr. 2017.

[17] Y. Liu, Y. Pan, and F. Yao, "A modified adaptive filtering acquisition method for PN code with data modulation," *IEEE Commun. Lett.*, vol. 15, no. 8, pp. 869–871, Aug. 2011.

[18] Y. Shen, Y. Wang, Z. Peng, and S. Wu, "Multiple–access interference mitigation for acquisition of code–division multiple–access continuous–wave signals," *IEEE Commun. Lett.*, vol. 21, no. 1, pp. 192–195, Jan. 2017.

[19] S. Blunt and K. Gerlach, "Multistatic adaptive pulse compression," *IEEE Trans. Aerosp. Electron. Syst.*, vol. 42, no. 3, pp. 891–903, Jul. 2006.

[20] R. Prasad and S. Hara, "An overview of multi-carrier CDMA," in *Proc. Int. Symp. Spread Spectr. Techn. Appl.*, Mainz, Germany, Sep. 1996, pp. 107–114.

[21] J. Chen, J. Benesty, and Y. Huang, "Time delay estimation in room acoustic environments: An overview," *EURASIP J. Adv. Signal Process.*, vol. 2006, no. 1, Dec. 2006, Art. no. 026503.

[22] N. Letzepis and A. Grant, "Bit error rate estimation for turbo decoding," *IEEE Trans. Commun.*, vol. 57, no. 3, pp. 585–590, Mar. 2009.

[23] S. Wang, Z. Li, and Y. Zhang, "Application of optimized filters to two–dimensional sidelobe mitigation in meteorological radar sensing," *IEEE Geosci. Remote Sens. Lett.*, vol. 9, no. 4, pp. 778–782, Jul. 2012.

[24] C. O'Driscoll, "Performance analysis of the parallel acquisition of weak GPS signals," Ph.D. dissertation, Dept. Elect. Electron. Eng., Nat. Univ. Ireland, Galway, Ireland, 2007.

YUYAO SHEN received the bachelor's and Ph.D. degrees from the School of Information and Electronics, Beijing Institute of Technology, Beijing, China, in 2011 and 2017, respectively. She currently holds a postdoctoral position at the Academy of Opto-Electronics, Chinese Academy of Sciences. Her research interests include space-flight TT&C and space communication, specifically, spread-spectrum signal processing.

YING XU received the Ph.D. degree in signal processing from the Beijing Institute of Technology, China, in 2009. She is currently a Research Professor, a Doctoral Supervisor, and the Vice Director of the Navigation Technology Research Laboratory, Academy of Opto-Electronics, Chinese Academy of Sciences. Her research interests include satellite-navigation technology and its augmentation, and multisource fusion localization theory and methods.